DOI: 10.1534/genetics.106.056721

The Molecular Identities of the *Caenorhabditis elegans* Intraflagellar Transport Genes *dyf-6*, *daf-10* and *osm-1*

Leslie R. Bell,[1] Steven Stone,[2] John Yochem, Jocelyn E. Shaw and Robert K. Herman

Department of Genetics, Cell Biology, and Development, University of Minnesota, Minneapolis, Minnesota 55455

Manuscript received February 3, 2006
Accepted for publication April 28, 2006

ABSTRACT

The *Caenorhabditis elegans* genes *dyf-6*, *daf-10*, and *osm-1* are among the set of genes that affect chemotaxis and the ability of certain sensory neurons to take up fluorescent dyes from the environment. Some genes in this category are known to be required for intraflagellar transport (IFT), which is the bidirectional movement of raft-like particles along the axonemes of cilia and flagella. The cloning of *dyf-6*, *daf-10*, and *osm-1* are described here. The *daf-10* and *osm-1* gene products resemble each other and contain WD and WAA repeats. DYF-6, the product of a complex locus, lacks known motifs, but orthologs are present in flies and mammals. Phenotypic analysis of *dyf-6* mutants expressing an OSM-6::GFP reporter indicates that the cilia of the amphid and phasmid dendritic endings are foreshortened. Consistent with genetic mosaic analysis, which indicates that *dyf-6* functions in neurons of the amphid sensilla, DYF-6::GFP is expressed in amphid and phasmid neurons. Movement of DYF-6::GFP within the ciliated endings of the neurons indicates that DYF-6 is involved in IFT. In addition, IFT can be observed in dauer larvae.

INTRAFLAGELLAR transport (IFT) is the regular movement of raft-like particles in both directions along the axonemes of flagella and cilia. A pioneering analysis in the alga *Chlamydomonas reinhardtii* led to the biochemical identification of what have been termed complex A and complex B components of IFT particles (for review, see Rosenbaum and Witman 2002; Cole 2003; Scholey 2003). Six proteins have been assigned to complex A and 10 to complex B. Kinesin-2 family members are responsible for anterograde movement of the particles, while retrograde movement is under the direction of an IFT dynein. In what is thought to reflect a contribution of material to the tip of the axoneme and therefore to the assembly and maintenance of the flagellum, the morphology of the IFT particles changes at the tip of the axoneme. Consistent with this notion, mutations that affect components of the IFT particles confer aberrant flagella. IFT is also thought to transport flagellar components necessary for sensation of environmental molecules.

Although the nematode *Caenorhabditis elegans* lacks flagella, it has neurons that contain nonmotile cilia (White *et al.* 1986) that are known to undergo IFT (for review, see Cole 2005). Some of these sensory neurons belong to the left–right pair of amphid sensilla in the head and others belong to the left–right pair of phasmid sensilla in the tail. The cilia are present in the dendritic endings of the neurons of these sensilla. The endings of several amphid dendrites unite into a compact bundle and penetrate the body cuticle by means of a specialized channel, thereby allowing exposure of the dendrites to the environment. Mutations that alter chemotaxis (the Che phenotype), the ability to avoid high osmolarity (Osm), the ability to form dauer larvae (Daf defective), and the ability of the phasmid and certain amphid neurons to take up fluorescent dyes from the environment (Dyf), which are all processes that seem to require exposure of dendrites to the environment, are known in some cases to affect the morphology of the amphid and phasmid cilia (Lewis and Hodgkin 1977; Albert *et al.* 1981; Perkins *et al.* 1986). Consistent with an effect on cilia, some of these mutations affect genes that encode counterparts of complex A or B components of the Chlamydomonas IFT (for review, see Cole 2003). Moreover, on the basis of fusions of GFP with OSM-6, OSM-1, DAF-10, and others, IFT has been demonstrated for the cilia of the dendritic endings of the amphids and phasmids in *C. elegans* (Orozco *et al.* 1999; Signor *et al.* 1999; Qin *et al.* 2001; Blacque *et al.* 2005; Ou *et al.* 2005a,b).

The complex structure of cilia and flagella raises the question of the total number of the components involved in their assembly and maintenance. Recently, a flagellar or ciliary proteome, the "flagellar apparatus basal body proteome," was derived by comparing

Sequence data from this article have been deposited with the EMBL/GenBank Data Libraries under accession nos. DQ360810–DQ360813, DQ365983, and DQ365984.

[1]*Corresponding author:* Department of Genetics, Cell Biology, and Development, University of Minnesota, Room 6-160 Jackson Hall, 321 Church Street SE, Minneapolis, MN 55455. E-mail: bellx035@umn.edu

[2]*Present address:* Myriad Genetics, Salt Lake City, UT 84092.

protein sequences shared by humans and Chlamydomonas, both of which have such structures, after exclusion of proteins shared with Arabidopsis, which lacks them (Li *et al.* 2004). The proteome is composed of 688 protein species and includes those known from biochemical and genetic studies to be components of the IFT particles.

Gene products that affect the uptake of fluorescent dyes in *C. elegans* correlate well with the flagellar apparatus basal body proteome of Chlamydomonas (Li *et al.* 2004). OSM-1 and DAF-10, for example, have unambiguous orthologs in the proteome. Consistent with that finding, the dendritic endings of the amphid neurons in *osm-1* and *daf-10* mutants are known from ultrastructural analyses to have foreshortened cilia and other aberrancies (Lewis and Hodgkin 1977; Albert *et al.* 1981; Perkins *et al.* 1986), and, as mentioned above, OSM-1::GFP and DAF-10::GFP undergo IFT (Signor *et al.* 1999). The cloning of *osm-1* and *daf-10*, which permitted the IFT studies, is reported herein.

The cloning of the gene *dyf-6* on the basis of the Chlamydomonas proteome is also reported here. This gene, mutations in which confer Che, Daf, and Dyf phenotypes (Starich *et al.* 1995), has implications for IFT and the function of sensory cilia in *C. elegans*.

MATERIALS AND METHODS

Genetic strains and markers: Descriptions of the genetic markers are available at http://www.wormbase.org. The *m175* and *mn346* alleles of *dyf-6*, the *m530*, *m538*, and *p816* alleles of *osm-1*, and the *m534*, *p821*, and *e1387* alleles of *daf-10* have been described genetically (Starich *et al.* 1995). *m530*, *m538*, and *m534* arose spontaneously in a strain, RW7097, that has a high rate of Tc1 transposition, and were provided by D. Riddle, University of Missouri. *mnIs17* is an integrated transgenic array that confers expression of OSM-6::GFP in the amphid and phasmid neurons and that therefore allows visualization of the gross morphology of the dendritic endings of these neurons (Collet *et al.* 1998). The effect of *dyf-6* on the morphology of the amphid and phasmid neurons was determined by comparing the OSM-6::GFP pattern in the strains SP2409, *unc-36(e251); dyf-6(m175); mnIs17[osm-6::gfp; unc-36(+)]*, and SP2733, *unc-36(e251); dyf-6(mn346); mnIs17*, with the pattern in the *dyf-6(+)* strain SP2453, *ncl-1(e1865) unc-36(e251); mnIs17*.

Assay of dye uptake: Stock solutions (~10 mm) of 3,3′-dioctadecyloxacarbocyanine (DiO) (obtained from the Sigma Chemical, St. Louis) or of 1,1′-dioctadecyl-3,3,3′,3′-tetramethylindodicarbocyanine (DiD) (Invitrogen/Molecular Probes, Eugene, OR) in *N,N*-dimethylformamide were stored at 4°. Uptake of the dyes by living worms was assayed essentially as described (Herman and Hedgecock 1990). Briefly, worms were immersed at room temperature for 2–5 hr in 30 μl of the dyes, which had been diluted to ~20 μM with half-strength M9, and then transferred to drops of M9, which contained 10 mm levamisole hydrochloride (Sigma Chemical), on 5% Noble agar pads. Animals were examined with a 100× objective for the filling of the phasmid neurons and of 12 amphid neurons, ASHR, ASIR, ADLR, ASJR, ASKR, AWBR, ASHL, ASIL, ADLL, ASJL, ASKL, and AWBL. Of the total 24 amphid neurons in the organism, these 12 are the ones competent to fill with fluorescent dyes (Starich *et al.* 1995), and throughout this work the term "amphid neuron" will refer only to one or more of the aforementioned cells.

Micro-injection of DNA: Following micro-injection (Mello and Fire 1995) of phage λ DNA, cosmid DNA, or long-range PCR products, transgenic animals were identified on the basis of the co-injection of either of the transformation markers pRF4, which expresses *rol-6(su1006)* (Mello *et al.* 1991), or pTG96, which expresses *sur-5::gfp* (Yochem *et al.* 1998). Phage λ genomic clones were provided by Chris Link (University of Colorado, Boulder, CO), and cosmid clones by Alan Coulson (The Sanger Institute, Hinxton, England). Primers for long-range PCR products were designed on the basis of the physical map and DNA sequence of the relevant regions of the genome, which are available at http://www.wormbase.org. The long-range PCR products were generated with the Expand Long Template PCR system (Roche Diagnostics, Indianapolis). For *dyf-6*, the primers for the PCR product designated 1040 were LRB-395 (cacaatagctggatcgtggaaatcgtcg) and LRB-403 (ttgaactaccagcaggagaagctcaacc).

Molecular techniques and DNA sequence analysis: Insertions and subsequent excisions of the Tc1 transposable elements in *daf-10* and *osm-1* were determined by Southern blotting and by DNA sequencing. For determination of the DNA sequence changes associated with the ethyl methanesulfonate (EMS) alleles *e1387* and *p821* of *daf-10* (Perkins *et al.* 1986; Starich *et al.* 1995) and *m175* of *dyf-6* (Starich *et al.* 1995), mutant homozygotes were used to generate PCR products representing the exons and small parts of the flanking introns. Sequences of both strands were determined and compared with wild-type sequences by the BLAST program (Altschul *et al.* 1997). The DNA sequence of the PCR fragments was determined *en masse* at the Advanced Genetic Analysis Center (University of Minnesota).

Analysis of mRNA: The true 5′ ends of the *dyf-6* and *daf-10* mRNAs were determined with the FirstChoice RNA ligase-mediated rapid amplification of cDNA ends (RLM-RACE) kit (Ambion, Austin, TX). cDNA was generated from total RNA that had been isolated from mixed-staged populations of N2 worms by means of TRIzol (Invitrogen, San Diego). The 3′ ends of both genes were also determined by means of the kit. For both ends, gene-specific primers were used in combination with primers provided with the kit. All internal splice sites were verified during the RACE analysis or by additional RT–PCR and, in the case of *daf-10*, by an analysis of three partial cDNA clones from the library of S. Kim and R. Horvitz and the library of R. Barstead and R. Waterston. These clones identified exon 8 through the 3′ end. The mRNA of *osm-1* was determined by means of two cDNA clones obtained from the libraries cited above, which identified exon 13 through the 3′ end. These *osm-1* cDNAs were extended 5′ using multiple rounds of RT–PCR with primers to potential upstream exon sequences that lay within the limits of the rescuing DNA. The 5′ end was identified using RNAse protection, RACE, and RLM-RACE. For all genes, the amino acid sequences that had been deduced for the gene products on the basis of the analysis of mRNA were compared and aligned with various orthologs by the PileUp program [Wisconsin Package Version 10.3, Accelrys (CGC), San Diego].

Genetic mosaic analysis: Mosaics were generated from a strain transgenic for an extrachromosomal array containing a functional copy of *dyf-6* (PCR1040) and a cell-autonomous marker that indicates inheritance of the array. Because the cell-autonomous marker, SUR-5::GFP, fluoresces green, as does DiO, dye filling was assessed with DiD, which fluoresces red instead of green. A standard GFP filter set was used for the examination of the nuclear expression of SUR-5::GFP; for uptake of DiD, a standard Texas Red set was used. No overlap was seen between the filter sets, and a comparative study

demonstrated that DiD is taken up by the same cells as is DiO.

The amphid neurons (and their lineage designations) that take up DiD and DiO (Starich *et al.* 1995) are, on the right, ASHR (ABprpaappaa), ASIR (ABpraapapppa), ADLR (AB praaapaad), ASJR (ABpraaappppa), ASKR (ABpraaaapppa), and AWBR (ABpraaappap), and on the left, ASHL (ABplpaap paa), ASIL (ABplaapapppa), ADLL (ABalpppaad), ASJL (ABalpppppppa), ASKL (ABalpppapppa), and AWBL (AB alpppppap). Plates were examined with a dissecting microscope equipped with a Hg lamp for GFP mosaics, which were removed, treated with DiD, and then analyzed with a compound microscope for uptake of DiD and for detailed assessment of the mosaicism.

Construction and microscopy of the DYF-6::GFP reporter: PCR was used to amplify a 9-kb fragment using wild-type genomic DNA as the template and the primers LRB-424 (tttcaaaggtggagtatggccagtggag) and LRB-378 (gacgcagagaa tgtgcatgcacagtttg). The PCR product was cut at two sites with *Cla*I to create a 7-kb fragment and subcloned into the *Cla*I site of pBlueScript(−); the *Not*I site of the vector was deleted by cutting with *Sac*II and *Sma*I, making ends flush with T4 DNA polymerase, and then religating. A 1-kb *Not*I DNA fragment encoding GFP was excised from pPD102.3 (provided by A. Fire, Stanford University) and inserted in frame at an *Eag*I site in the tenth and final exon of the gene. A strain, SP1712, homozygous for *dyf-6(m175)*, was micro-injected with the final plasmid, pLRB104, at a concentration of 90 ng/μl and with pRF4 at 45 ng/μl. Although transgenic lines differed in brightness of green fluorescence, all exhibited the same cell-specific pattern of expression of the construct. The strains SP2730 and SP2731, which have extrachromosomal arrays independent of each other, were established from two of the brightest lines. To examine IFT, adults from these strains were chosen because of their large size and transferred to drops of M9 on 5% Noble agar pads. The M9 contained 10 mm levamisole hydrochloride for thorough anesthesia (Signor *et al.* 1999). DYF-6::GFP was examined with a 100× objective of an Axioplan 2 microscope (Carl Zeiss, Thornwood, NJ), which was equipped with a CCD camera and the image software AxioVision 4.2 (Carl Zeiss). A temperature-controlled stage was not used; ambient temperature was ~25°. Time-lapse images were taken every 0.5 sec. The rate of IFT was determined by measuring five sets of sequential still images in which a particle could be followed for at least three frames. Movies were generated using Media Cleaner Pro 4.0 (Terran Interactive).

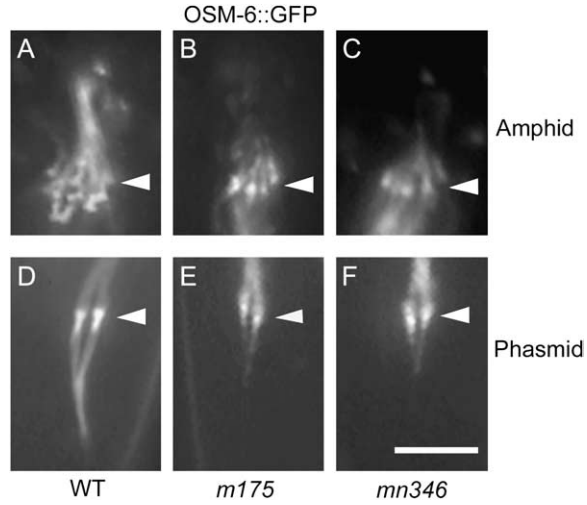

Figure 1.—Aberrant pattern of OSM-6::GFP in *dyf-6* mutants. (A) The wild-type pattern of an amphid sensillum in *dyf-6(+)*. Note the tapering of the fluorescence into a single unit toward the anterior tip of the animal (anterior is up in all micrographs). The single unit corresponds to the channel of the ciliary endings through the amphid sheath and body cuticle. The transition zone between the dendritic bodies and the dendritic endings is indicated with an arrowhead. (B) An abnormal pattern typically seen with the *dyf-6(m175)* mutation. Note the failure of the fluorescence to extend to the tip of the animal. (C) The other mutation, *dyf-6(mn346)*, confers a similar defect at the anterior end of the amphid neurons. (D) Expression of OSM-6::GFP in a phasmid sensillum in the tail of a *dyf-6(+)* animal. The transition zone at the junction between the dendritic bodies and the ciliated endings that penetrate the cuticle is indicated with an arrowhead. (E) A much shorter region of fluorescence below the arrowhead indicates aberrant, apparently truncated, dendritic endings of the phasmid neurons in a *dyf-6(mm175)* animal. (F) Aberrant endings are also apparent in *dyf-6(mn346)* mutants. Bar, 5 μm.

RESULTS

Aberrant dendritic endings of the amphid and phasmid neurons in *dyf-6* mutants: The cilia of both *daf-10* and *osm-1* mutants have an aberrant, foreshortened morphology (Lewis and Hodgkin 1977; Albert *et al.* 1981; Perkins *et al.* 1986). The dye-filling defect of *dyf-6* mutants indicates that the dendritic endings of their amphid and phasmid neurons may also be defective. This possibility was examined by constructing strains that are either wild type for *dyf-6* or homozygous for the *m175* or *mn346* alleles and that have a transgenic array that expresses an OSM-6::GFP reporter (Collet *et al.* 1998) in the amphid and phasmid neurons.

The pattern of OSM-6::GFP in the amphid dendrites of a *dyf-6(+)* strain, SP2453, agrees with the pattern seen by others in a nonmutant background (Signor *et al.* 1999): there is a tapering of the fluorescence at the dendritic endings into a tight band as one moves toward the anterior tip of an animal (Figure 1A). This pattern of fluorescence is consistent with the formation of a compact bundle of ciliated endings as they enter the amphid sheath and penetrate the body cuticle of either the left or the right amphid sensillum. In electron micrographs of wild-type worms, the tapering of the dendrites of the amphids becomes pronounced at the transition zone between the bodies of the dendrites and their specialized endings, which contain the cilia (Perkins *et al.* 1986), and it is presumed here that the tapering of fluorescence corresponds to what has been seen at the ultrastructural level. In *dyf-6* mutants, in contrast, fluorescence fails to extend as far anterior as in wild type (Figure 1, B and C). The correlation between cilia length and the OSM-6::GFP pattern has been described (Collet *et al.* 1998) and the pattern seen here is consistent with cilia that are foreshortened, lacking the distal part, as seen in electron micrographs of *osm-1*, *daf-10*, and several other mutants (Lewis and Hodgkin 1977;

Albert *et al.* 1981; Perkins *et al.* 1986). Verification of truncated cilia would, however, require observations at the ultrastructural level. The dendritic endings of the phasmid neurons also appear to be foreshortened in *dyf-6* mutants (Figure 1, E and F) relative to that of *dyf-6(+)* animals (Figure 1D).

The dye-filling defect of *dyf-6* mutants is completely penetrant (Starich *et al.* 1995). Likewise, the morphology, as shown by OSM-6::GFP, of the defective dendritic endings of the amphid and phasmid neurons showed little variation among the animals. It is therefore reasonable to conclude that aberrant, apparently foreshortened cilia account for the failure of the amphid and phasmid neurons to fill with dye in these mutants.

Cloning of the *dyf-6* gene: A proteome of cilia and basal bodies has been generated by genomic comparisons among three species, Chlamydomonas and humans, which contain such structures, and Arabidopsis, which lacks them (Li *et al.* 2004). The positions of *C. elegans* orthologs of the proteome were located on the physical map by means of WormBase and then correlated with the positions of uncloned genes whose mutant phenotypes indicate that they are candidates for affecting the ciliary dendrites of the amphids (Starich *et al.* 1995). On the basis of the correlation of the physical and genetic maps, three of the orthologs of the proteome were considered candidates for being *dyf-6 X*. The first indication that one of these, F46F6.4, may be *dyf-6* was a failure to obtain a PCR product for this gene when DNA from *mn346*, which arose from a mutator strain (Starich *et al.* 1995) and therefore is likely to have an insertion of a transposable element, was used as the template. In contrast, use of *dyf-6(m175)* DNA as the template resulted in a product of wild-type size. DNA sequencing of the PCR product demonstrated a C-to-T transition that changed a CGA codon to a stop codon in the fifth exon of the short transcript (*dyf-6b*) relative to the wild-type sequence present in WormBase (Figure 2). The DNA sequence of the corresponding product from wild-type template was in complete agreement with the sequence present in WormBase. Confirmation that F46F6.4 is *dyf-6* was obtained by rescue of the dye-filling defect in worms transgenic for an extrachromosomal array that contains the PCR fragment 1040, which is specific for the gene (Figure 2).

The *dyf-6* gene product: RLM-RACE together with 3′-RACE demonstrated that *dyf-6* is a complex locus involving overlapping transcripts, covering a 6.8-kb genomic region, that differ at both the 5′ and 3′ ends (Figure 2). The two WormBase-designated genes F46F6.3 and F46F6.4 (*dyf-6b*) are adjacent and each produces its own transcript as diagrammed in Figure 2, encoding 161 and 320 amino acids, respectively. In a minor alternatively spliced form of F46F6.4 (*dyf-6c*), an additional intron is present within the third exon to give a mini-exon of 7 bp followed by a 66-bp intron to form a transcript encoding 298 amino acids.

Figure 2.—The *dyf-6* gene. Diagrammed are the overlapping transcripts of the *dyf-6* complex locus. The location of the *dyf-6(m175)* mutation is shown. At the bottom are shown the rescuing PCR fragment 1040 and the DYF-6::GFP plasmid.

In addition, there is a much larger transcript, which is readily detectable by both 3′-RACE and RLM-RACE, in which the F46F6.3 and F46F6.4 transcription units are fused into a longer form (*dyf-6a*) encoding 474 amino acids. Nevertheless, the smaller transcripts, *dyf-6b* and *dyf-6c*, appear sufficient for *dyf-6* function since the PCR fragment 1040, which lacks part of F46F6.3, is sufficient for rescue, at least when overexpressed from extrachromosomal arrays. The function, if any, of the largest transcript, *dyf-6a*, remains unknown. Although many of the ciliary genes of *C. elegans* have a promoter motif, termed the X-box, upstream of the translational start site (Efimenko *et al.* 2005), no sequence exactly matching the "refined" (GTHNYYATRRNAAC) or the "average" consensus (RTHNYYWTRRNRAC) is found upstream of either of the two identified start sites of *dyf-6*. However, the sequence GTCTCCATGGTTTAC, which differs from the refined consensus by one nucleotide, is present 89 bp upstream of the ATG of *dyf-6a*. Two sequences found 36 and 142 bp upstream of the ATG of *dyf-6b*, CTTCCAC TAATAAC and AACCTCAGGAAAAC, differ at three nucleotides from the refined consensus.

The alignment of the amino acid sequence predicted for the short, rescuing version of the gene DYF-6B with orthologs from human and Drosophila is shown in Figure 3. The three proteins show significant similarity throughout the protein sequence. Many of the gaps may be due to the provisional nature of the Drosophila prediction, which is lacking EST data. There are no known sequence motifs. Notably, however, the amino terminus contains two acidic regions. The DYF-6 acidic region spanning amino acids 6–13 is shared with the human and Drosophila proteins. A larger acidic region, at DYF-6 residues 78–94, is also present in the human protein.

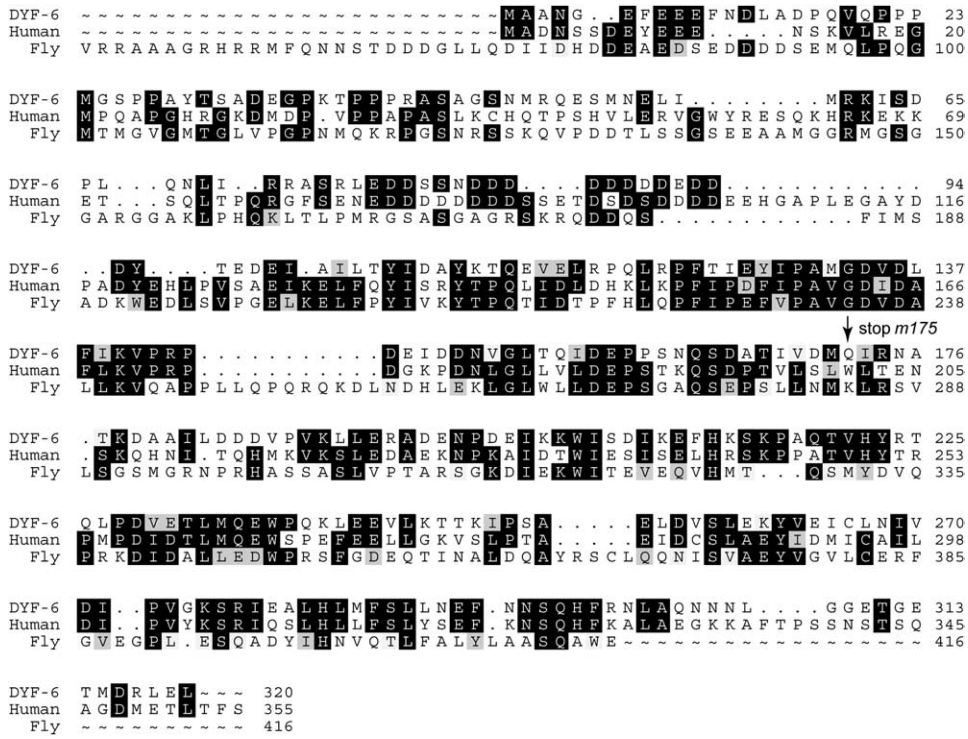

FIGURE 3.—Comparison of DYF-6B with orthologs from human (GenBank NP 06538) and fly (*Drosophila melanogaster*, GenBank NP 609890). The N-terminal 50 amino acids of the Drosophila protein are not shown, as they contain no sequence similarity. We note that the Drosophila gene is a prediction, unsupported by EST data. The position of the *dyf-6(m175)* mutation is indicated.

An analysis of animals mosaic for *dyf-6*: The effect of *dyf-6* on the dendrites of the amphid neurons could be explained by a requirement for the gene in the amphid neurons themselves, in the socket or sheath cells that support the dendrites of these neurons (PERKINS *et al.* 1986) or in both the neurons and their support cells. Because of the junction that is formed with the body cuticle, a requirement in the hypodermis, the source of this cuticle, is also possible. To investigate the cellular requirement of *dyf-6*, genetic mosaics segregating from SP2732, a strain having the genotype *dyf-6(m175); mnEx172[dyf-6(+) (PCR1040); sur-5::gfp]*, were analyzed for their ability to take up the fluorescent dye DiD from the environment.

The phasmid and the 12 amphid neurons that are competent to fill with fluorescent dyes all filled with DiD in all AB(+) P_1 (−) mosaics. In contrast, none of these neurons filled in 11 of 11 AB(−) P_1 (+) mosaics. These observations are as expected, because all of the components of the amphid and phasmid sensilla descend from AB. Closer examination of the cellular requirement of *dyf-6* took advantage of the cell lineage of certain of the amphid neurons relative to the amphid sheath and socket cells. All of the amphid sheath and socket cells descend from ABp, one of the granddaughters of the zygote. On the right side of the animal all of the dye-filling amphid neurons also descend from ABp, but a difference in lineage exists for the corresponding amphid neurons on the left side: although two of them, ASHL and ASIL, descend from ABp, four of them, ADLL, ASJL, ASKL, and AWBL, descend from ABa, the sister of ABp (SULSTON *et al.* 1983). Thus, in an ABa(+) ABp(−) mosaic all of the amphid sheath and socket cells will lack a wild-type copy of the *dyf-6* gene, as will all of the amphid neurons on the right side. In contrast, four of the amphid neurons on the left, those that descend from ABa, will have wild-type copies of *dyf-6*, which are present on the extrachromosomal array.

The pattern of dye filling clearly indicates that *dyf-6* is not required in the amphid sheath or socket cells: in eight of eight ABa(+) ABp(−) mosaics, mosaics in which all of the amphid sheath and socket cells are minus for the array, the ABa amphid neurons nevertheless readily filled with DiD. In contrast, none of the amphid neurons on the right filled, which is consistent with their descent from ABp. The mosaics therefore indicate that *dyf-6* must function within the amphid neurons themselves for uptake of DiD, a notion also supported by the pattern of expression of a functional DYF-6::GFP fusion construct, as described below. The function of *dyf-6* was not, however, cell autonomous: in seven of the eight ABa(+) ABp(−) mosaics, all of the amphid neurons on the left side took up the dye, even the two that descended from ABp and were therefore minus for the array; in the one exceptional mosaic, ASIL (ABplaapapppa) did not fill. It therefore appears that *dyf-6* does not function cell autonomously for uptake of DiD. Instead, the function of the gene is autonomous at the level of the amphid dendritic bundle.

IFT of DYF-6::GFP in amphid and phasmid neurons: To determine whether or not DYF-6 might undergo IFT in the dendritic endings of the phasmid and dye-filling amphid neurons, an in-frame fusion of *dyf-6* and *gfp* was created. The translation product predicted for the short

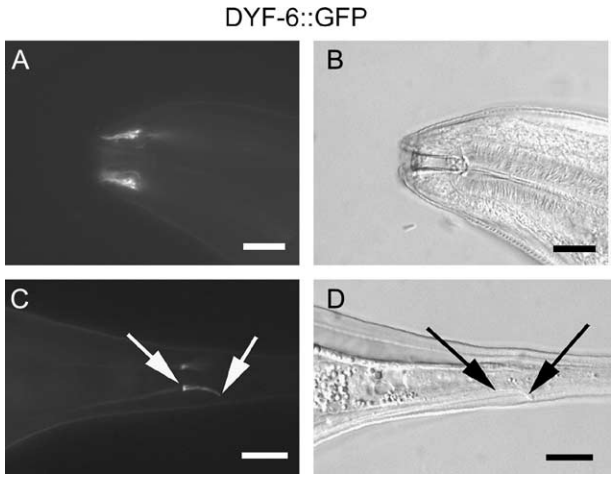

FIGURE 4.—Expression of DYF-6::GFP. (A) DYF-6::GFP is in the dendritic endings of amphid neurons. As for OSM-6::GFP, note the anterior tapering of the endings. Both the left and the right amphid sensilla are visible in this dorsal–ventral view. (B) The corresponding Nomarski image of the animal in A. (C) Expression of DYF-6::GFP in the dendritic endings, delineated by arrows, of phasmid neurons. The view is slightly dorsal–ventral, and the other phasmid sensillum can also be seen. (D) The corresponding Nomarski image of C. Bars, 10 μm.

form, which can rescue the nonsense allele of *dyf-6*, has 320 amino acids, and *gfp* was fused in frame between the 253rd and 254th codons of the gene in a plasmid construct, pLRB104, that has a nearly similar amount of 5′ and 3′ flanking DNA as is present on the rescuing PCR fragment 1040 (Figure 2). Micro-injection of *dyf-6(m175)* homozygotes with 90 ng/μl of pLRB104 together with 45 ng/μl of pRF4, which expresses *rol-6(su1006*dm*)* (MELLO *et al.* 1991), resulted in transgenic worms that were robustly rescued for the uptake of DiD or DiO by the phasmid neurons and by the 12 dye-filling amphid neurons, demonstrating that the *dyf-6::gfp* construct is functional. On the basis of transgenic lines that arose independently of each other, expression of DYF-6::GFP is restricted to a few cells from hatching to adulthood. Of particular note, DYF-6::GFP is consistently expressed in the cell bodies, dendritic bodies, and dendritic endings of the phasmid neurons (Figure 4C). Expression was also very evident in the dendritic bodies and endings of the amphid sensilla (Figure 4A). DYF-6::GFP was faintly and irregularly expressed in the cell bodies of the dye-filling amphid neurons. A cell body could fill with DiD even in cases in which DYF-6::GFP was not seen in that cell body. It is not known if this reflects mosaicism of the transgenic array or expression of the GFP construct below the level of detection. Expression of DYF-6::GFP was also seen in the hypodermis and in several neuronal cell bodies in the region of the inner labial cell bodies. Finally, expression can be seen in a lateral neuronal cell body in the region of the PDE cell body in older larvae and adults.

For both the amphid and phasmid neurons, the greatest intensity of DYF-6::GFP was in the transition zone between the dendritic bodies and their ciliary endings (Figure 4). Of particular note, anterograde and, to a lesser extent, retrograde movement of GFP particles could be seen along the length of the dendritic endings of both the amphid (supplemental movie at http://www.genetics.org/supplemental/) and phasmid neurons. In the amphid neurons, the particles moved in the anterograde direction over the combined middle and distal segments of the ciliary axoneme at 0.9 ± 0.1 μm/sec (Figure 5). This rate falls within the range described for IFT of OSM-6::GFP (SNOW *et al.* 2004) of 0.68 μm/sec in the middle segment and 1.27 μm/sec in the distal segment. IFT could be seen prior to hatching and throughout postembryonic development and adulthood.

IFT of DYF-6::GFP in dauer larvae: Starvation and a high population density can induce a diapause, the dauer larva, which is capable of enduring harsh conditions (RIDDLE and ALBERT 1997). A return to more favorable conditions results in a molt to the fourth larval stage and a resumption of growth and development. Because an amphid neuron can affect exit from the dauer state (BARGMANN and HORVITZ 1991), it was of interest to determine whether or not the dendritic endings of the amphid neurons are of normal appearance and exhibit IFT in dauer larvae. Six dauer larvae from SP2730 were picked from plates exhausted of bacteria to NGM plates without bacteria, followed by a further incubation of 3 days. DYF-6::GFP was expressed in the cell bodies and in the dendritic bodies and endings of the dye-filling amphid neurons (Figure 6). Moreover, IFT could be easily seen in the dendritic endings, but there appeared to be fewer GFP particles undergoing IFT in the amphid bundles relative to that seen in non-dauer animals.

DYF-6::GFP was also expressed in the cell and dendritic bodies of the phasmid neurons in the six dauer larvae (the dendritic bodies were often kinked, as though their linearity had been affected by shrinkage of the body during formation of the dauer state). In four of the animals, DYF-6::GFP indicated that the phasmid neurons had proper dendritic endings, and IFT of the GFP could be easily seen in the endings. In the other two animals, however, DYF-6::GFP did not provide evidence for the existence of dendritic endings for the phasmid neurons, indicating that the endings might occasionally be severely retracted or modified in dauer larvae.

The occasional failure to see dendritic endings with DYF-6::GFP might mean that the phasmid neurons are no longer exposed to the environment in such animals. This assumption was independently assessed by examining dye filling in larvae of the wild-type N2 strain that had been in the dauer state for >3 days. Following immersion in 20 μM DiD for 3.5 hr, each of seven larvae exhibited robust filling of the axons, dendrites, and cell bodies of the amphid neurons that are known to fill with

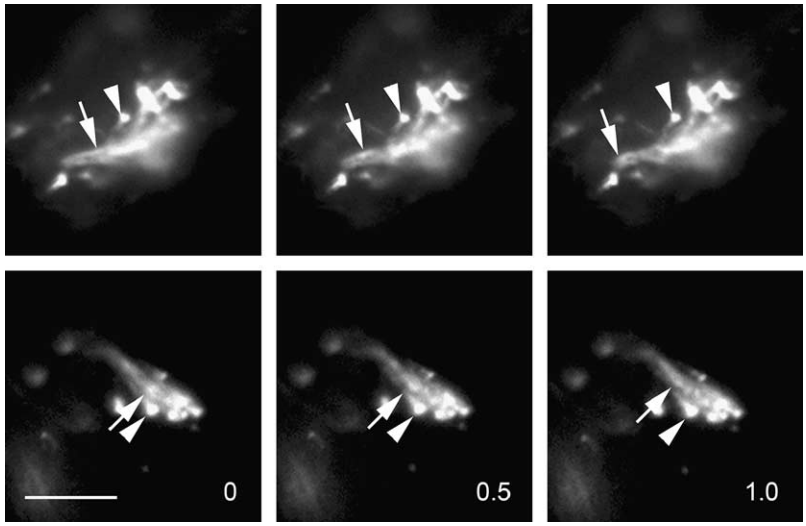

FIGURE 5.—Anterograde IFT of DYF-6::GFP in the amphid neurons. Time-lapse images taken at 0.5-sec intervals show the anterograde movement of DYF-6::GFP (arrow) relative to an immobile particle at the transition zone (arrowhead). Bar, 5 μm.

DiD in non-dauer larvae. In only one of the seven animals, however, did the phasmid neurons fill robustly; in three of the animals there was no evidence of filling; in the other three animals very weak filling could be seen in one of the phasmid sensilla, with no evidence for filling of the other.

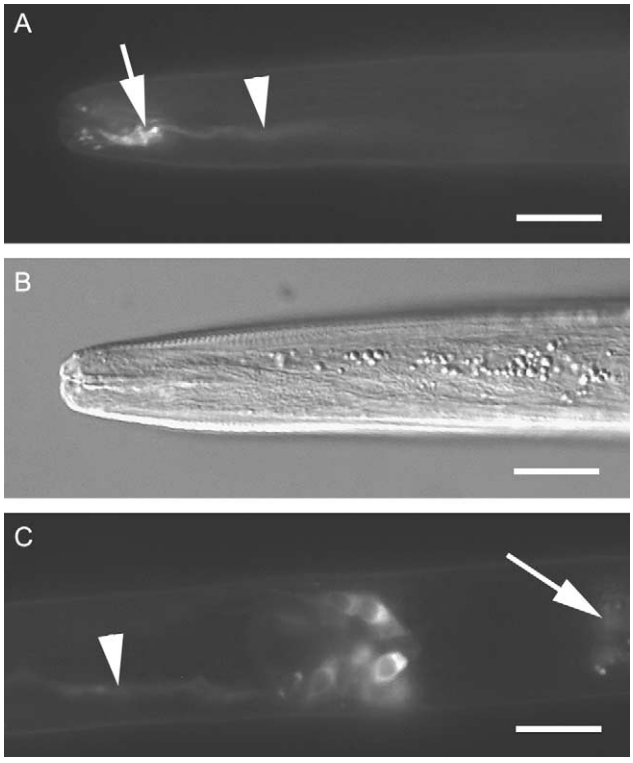

FIGURE 6.—Expression of DYF-6::GFP in amphid neurons of dauer larvae. (A) Accumulation of fluorescence in the dendritic endings of amphid neurons. An arrow marks the transition zone. Fainter fluorescence can be seen in the dendritic bodies (arrowhead). (B) The corresponding Nomarski image of A. (C) Dorsal–ventral view of bright fluorescence in the cell bodies of amphid neurons in another dauer larva. Fainter fluorescence can also be seen in dendritic bodies (arrowhead). An arrow delimits autofluorescent gut granules just posterior to the terminal bulb of the pharynx. Both specimens had been in the dauer state for >3 days. Bars, 10 μm.

Cloning of the *daf-10* gene: The *daf-10* gene was cloned on the basis of an allele, *m534::Tc1*, that arose spontaneously in a strain with a high rate of transposition of the Tc1 transposable element. Two independent revertants of *daf-10(m534)* were subsequently derived. Southern blot analysis with a probe specific for Tc1 led to the identification of a 2.1-kb *Eco*RI fragment unique to *m534* DNA; in particular, the fragment was not present in DNA isolated from either revertant. The transposon-tagged fragment led to isolation of a genomic λ-clone whose position on the physical map agreed well with the genetic mapping of *daf-10*. The λ-clone, which was presumed to contain the gene, maps to a cosmid clone, K09F8. Micro-injection of this clone led to the formation of extrachromosomal arrays that fully rescued the dye-filling defect of the *daf-10* mutant. Micro-injection of subclones of this cosmid indicated that *daf-10* corresponds to F23B2.4 (Figure 7A). Furthermore, F23B2.4 is altered in DNA isolated from

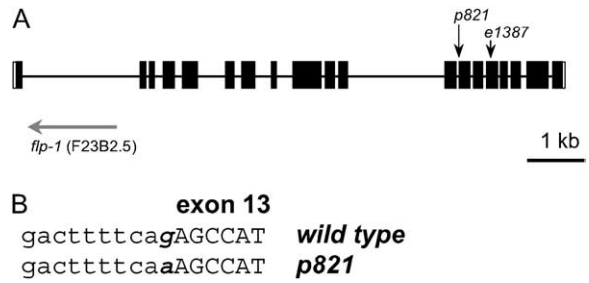

FIGURE 7.—The *daf-10* gene. (A) A schematic of the mRNA structure of *daf-10*. Another gene, *flp-1* (F23B2.5), is located within the first intron of *daf-10* (shaded arrow). The positions of the two sequenced *daf-10* mutations, *p821* and *e1387*, are shown. (B) The position of *daf-10(p821)*, which is a G-to-A transition at the 3′ splice site of exon 13. Intron sequence is in lowercase; exon is in uppercase.

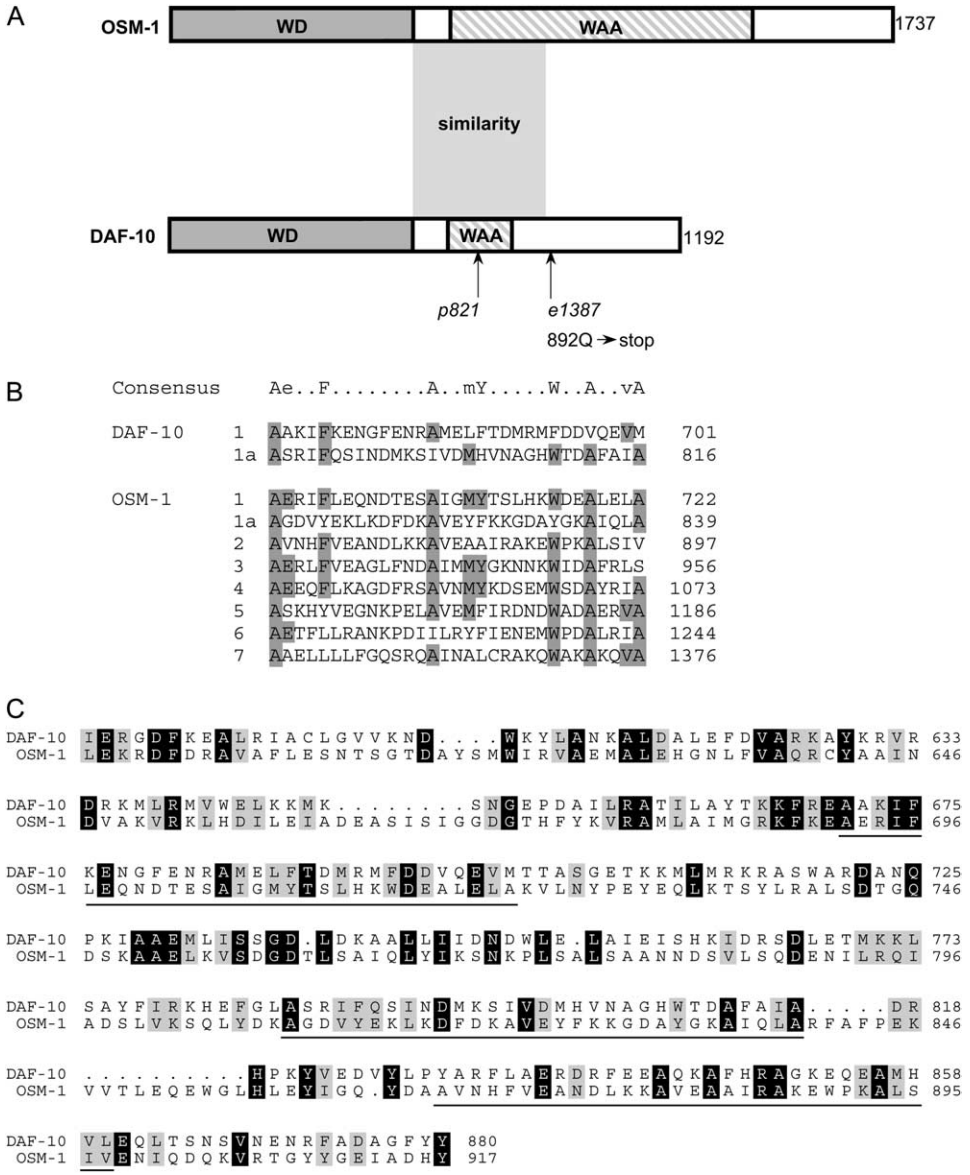

FIGURE 8.—DAF-10 and OSM-1 are structurally related. (A) Diagram of DAF-10 and OSM-1, showing regions of WD and WAA repeats. The most highly conserved region is indicated with the shaded box labeled "similarity," which corresponds to the sequence alignment in C. (B) DAF-10 and OSM-1 contain WAA repeats. The WAA consensus sequence is from PEDERSON *et al.* 2005. Identical amino acids are shaded. The WAA sequences present in OSM-1 are derived from the published alignment with Chlamydomonas IFT172 (PEDERSEN *et al.* 2005) with the exception of 1a, which we propose to be an additional WAA repeat. (C) Comparison of DAF-10 and OSM-1 in the region of highest similarity. This alignment corresponds to the shaded region labeled "similarity" in A. The three WAA repeats in this region are underlined.

mutants that originated from EMS mutageneses: *p821* is a G-to-A transition at the 3′ splice site of exon 13 (Figure 7B) and *e1387* is a C-to-T transition that changes a CAA codon (amino acid 892, Q) to TAA in exon 15.

The mRNA consists of 19 exons (Figure 7A). The first intron, which is ~2 kb in length, contains the transcript of another gene, *flp-1* (F23B2.5), as identified in WormBase. Many of the ciliary genes of *C. elegans* have a promoter motif, which has been termed the X-box, upstream of the translational start site (EFIMENKO *et al.* 2005). Binding of this motif by the DAF-19 transcription factor is thought to regulate the expression of these genes. *daf-10* has a match (ATCTCCATAGCAAC) to the X-box consensus sequence (GTHNYYATRRNAAC) 77 bp upstream of the ATG. There is a 14-bp 5′ UTR.

DAF-10 contains WD and WAA repeats: The fact that DAF-10 corresponds to IFT122, a complex A IFT of Chlamydomonas, has been previously reported (QIN *et al.* 2001), in part on the basis of unpublished work of S. STONE and J. E. SHAW. The mRNA analysis described above has led, however, to an amendment of the original interpretation of the predicted amino acid sequence of the gene product at both the amino terminus and internally. The amended product contains 1192 amino acids. Computer analyses indicate that the amino-terminal part has seven WD repeats. Although WD repeats can be difficult to discern on the basis of amino acid sequence, an analysis by eye raises the possibility that DAF-10 actually has 11 tandem WD repeats and that they compose the first 597 amino acids of the protein (Figure 8A). This possibility is consistent with computer predictions that this region would primarily form β-sheets, a hallmark of WD repeats, whose secondary structure is reminiscent of the blades of a propeller (SMITH *et al.* 1999).

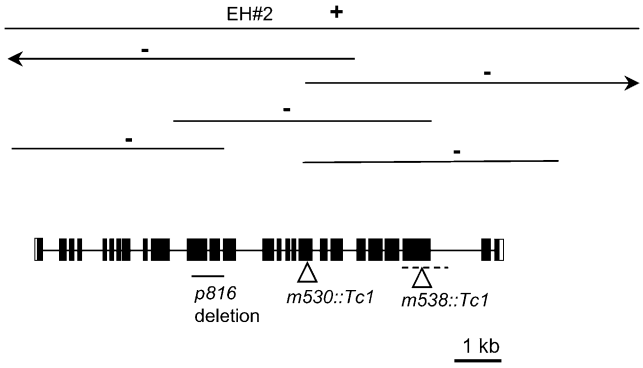

FIGURE 9.—Identification of the *osm-1* gene. Schematic of the λ-clone, EH#2, that rescues *osm-1* (indicated by +), and additional λ- and plasmid clones that do not rescue (indicated by −). The transcript structure is shown below. The positions of the three analyzed mutations are indicated; the dashed line shows the region within which *m538::Tc1* falls.

The predicted secondary structure changes abruptly to α-helices at the termination of the WD repeats. Eighty-four amino acids from the end of the WD repeats are two tandem copies of a second degenerate repeat (Figure 8B), the WAA repeat, which was first described in the IFT172 protein of Chlamydomonas (PEDERSEN *et al.* 2005). This repeat is expected to form α-helices, in contrast to the β-sheets of WD repeats.

Cloning of the *osm-1* gene: The cloning of *osm-1* was achieved on the basis of an allele that had arisen spontaneously in a Tc1 mutator background. Southern blot analysis of *m530::Tc1* and of two revertants led to the identification of genomic DNA that mapped to cosmid T27B1. Micro-injection of *osm-1* homozygotes with a genomic phage λ clone, EH#2, resulted in arrays that fully rescued the dye-filling defect of *osm-1(m530)* (Figure 9). This clone contains T27B1.1, which corresponds to *osm-1*. Southern blot analysis of alleles that arose in Tc1 mutator strains (*m530* and *m538*) or from EMS mutagenesis (*p816*, an ~600-bp deletion) confirmed the identity of the gene (Figure 9). The insertion site of *m530* was determined by DNA sequencing.

The *osm-1* mRNA is derived from 25 exons and contains 5305 nucleotides. As has been previously noted (EFIMENKO *et al.* 2005), there is a match (GCTACCAT GGCAAC) to the X-box consensus sequence (GTHN YYATRRNAAC) 86 bp upstream of the ATG. RLM-RACE analysis indicated that there are several transcription initiation sites to produce 5′ UTRs ranging from 20 to 29 bp.

OSM-1 and DAF-10 are structurally similar: It has been previously reported (COLE *et al.* 1998), in part on the basis of unpublished work of S. STONE and J. E. SHAW, that the gene product of *osm-1*, which is composed of 1737 amino acids, corresponds to IFT172, a complex B IFT of Chlamydomonas. OSM-1 is similar to DAF-10, having both WD and WAA repeats as well as a significantly similar central region (Figure 8A). Computer analyses of OSM-1 predict 7 copies of the WD motif, but as is the case for DAF-10 there may be 11, or possibly 12, tandem copies instead. These are followed by 8 tandem copies of the WAA repeat, in contrast to the 2 present in DAF-10 (Figure 8B). Immediately carboxyl terminal to the presumed end of the WD repeats is a region of sequence similarity between the two proteins (Figure 8, A and C). The end of the WD repeats and the start of the similarity correspond to a predicted switch from predominantly β-sheets to α-helices that extend throughout the similar region and all the WAA repeats of both proteins. The first part of the similar region does not correspond to known motifs. It then extends through the two WAA repeats of DAF-10 and the first two repeats of OSM-1. The similarity includes the third WAA repeat of OSM-1; however, the comparable region of DAF-10 does not appear to qualify as a WAA repeat by the consensus established by PEDERSON *et al.* (2005). The carboxyl-terminal regions of the two proteins lack sequence similarity.

DISCUSSION

Although *daf-10* contains another gene within its first intron, *daf-10* and *osm-1* are for the most part simple loci. In addition to having tandem WD repeats, the products of both genes have tandem WAA repeats (PEDERSEN *et al.* 2005), which have previously been termed "degenerate repeats" (COLE 2003). Only five genes in the *C. elegans* genome appear to encode proteins containing WAA repeats (J. E. SHAW, unpublished observations). These include CHE-11, the ortholog of Chlamydomonas IFT140 (QIN *et al.*, 2001); ZK520.1; and G54G7.4, a WD-containing protein that is present in the flagellar and basal body proteome and whose gene is preceded by an X-box. It is possible that the WAA repeat is present exclusively within components of IFT particles.

dyf-6 is part of a complex locus: in addition to two smaller, nearly identical mRNAs, a larger mRNA is also produced that contains the *dyf-6* open reading frame fused to the open reading frame of the adjacent gene upstream (F46F6.3). This work has concentrated on the shorter region of the *dyf-6* locus, because products of the short region confer full rescue of dye filling and because a fusion of it with GFP exhibits IFT. The smaller gene products also closely correspond in size with sequence-related proteins in other organisms; for example, the human ortholog is conserved throughout and begins at the same methionine. The ortholog in Drosophila, CG15161, is expressed in sensory cilia (AVIDOR-REISS *et al.* 2004) and shares sequence similarity only with the short forms. Moreover, the sequence specific to the F46F6.3 gene product appears to be confined to nematodes. The function, if any, of the larger *dyf-6* gene product remains unknown. The *m175* mutation should

affect not only the short forms but also the long form; however, we are unaware of defects caused by the mutation other than those associated with the amphid or phasmid sensilla.

With the exception of the hypodermis, the DYF-6::GFP construct was expressed only in a limited number of neurons. Those in the region of the inner labial neurons may correspond to the IL2 neurons, which, like the phasmid and dye-filling amphid neurons, are ciliated and are exposed to the environment (Ward *et al.* 1975; Ware *et al.* 1975). The pattern of expression of DYF-6::GFP appears to be a subset of that seen with OSM-6::GFP, which is expressed in nearly all (56 of 60) of the ciliated neurons of *C. elegans* (Collet *et al.* 1998). The expression pattern of DYF-3::GFP is also a subset of that seen with OSM-6::GFP (Murayama *et al.* 2005).

Although reporter constructs may not reliably indicate gene expression, movement of DYF-6::GFP along the cilia of the amphid and phasmid neurons provided compelling evidence that DYF-6 undergoes IFT. Anterograde movement appeared more apparent than retrograde movement. It is likewise easier to perceive anterograde movement of OSM-6::GFP, although retrograde movement can also be observed (Signor *et al.* 1999). It is not clear why it is more difficult to see retrograde movement. The intensity of the GFP does not increase at the tip of the cilia, which may indicate that much of the GFP is being degraded at the tip and therefore is less abundant in the retrograde direction. Alternatively, the GFP might be more diffuse during retrograde movement, as could be the case if those IFT particles contain less densely packed GFP. In addition to exchanging molecular motors, it is known that Chlamydomonas IFT particles undergo a change in structure at the tip, during which they become smaller (Piperno *et al.* 1998; Sloboda 2005).

On the basis of the expression pattern of OSM-6::GFP, *dyf-6* may encode a component of complex B IFT particles. As has been previously noted (Collet *et al.* 1998), the expression of OSM-6::GFP in the dendritic endings of amphid and phasmid neurons is reduced by mutation in *osm-1*, *che-2*, *che-13*, or *osm-5*, all of which encode complex B IFT components (Cole 2003); such a pattern is consistent with the foreshortened cilia seen in electron micrographs of these mutants (Lewis and Hodgkin 1977; Perkins *et al.* 1986). The expression of OSM-6::GFP in *dyf-6* mutants is similarly reduced in the dendritic endings. In contrast, mutation in *daf-10* or *che-11*, which encode complex A components, leads to thicker-than-wild-type patches of OSM-6::GFP expression in the endings of these neurons, which is not seen in *dyf-6* mutants. The pattern of OSM-6::GFP in *dyf-6* mutants therefore more closely resembles that of a complex B IFT component.

Consistent with the observation that DYF-6::GFP and OSM-6::GFP undergo IFT in the dendritic endings of the amphid neurons, genetic mosaic analyses of *osm-6* (Collet *et al.* 1998) and of *dyf-6* indicate that both genes are required only in the amphid neurons for the uptake of fluorescent dyes by these neurons. The *dyf-6* mosaics were, however, unusual in that the gene did not behave precisely cell autonomously. The *dyf-6* gene appears instead to be autonomous at the level of the amphid dendritic bundle: it appeared as though *dyf-6(+)* in four neurons was able to correct the dye-filling defect of two *dyf-6(−)* neurons in the same sensillum. In contrast, the *osm-6* gene, although there was one exceptional mosaic, behaved cell autonomously (Collet *et al.* 1998). An explanation for the discrepancy between the two analyses might be that DiD was used for the analysis of *dyf-6* but DiO for *osm-6*. Perhaps only some of the dendritic endings, those that are *dyf-6(+)*, need to be exposed to the environment for initial uptake of DiD. Once they have taken up the dye it is transferred to the *dyf-6(−)* dendrites or cell bodies farther posterior. This is a reasonable hypothesis, because it is known that dendritic endings of an amphid neuron need not penetrate the body cuticle for uptake of certain dyes: the left and right AWB neurons take up DiO (Starich *et al.* 1995) and DiD, but their endings are completely embedded in the amphid sheath and are therefore not directly exposed to the environment (Perkins *et al.* 1986). Thus, there must be transfer of the dye from the membrane of a neuron that is exposed to the environment to the membrane of the AWB dendrites.

The maintenance of IFT in amphid neurons of dauer larvae is perhaps to be expected. Although dauer larvae do not exhibit chemotaxis toward food, they can detect the presence of food, which stimulates an exit from the dauer state (Albert and Riddle 1983). Certain amphid neurons affect the entry into or exit from the dauer state (Bargmann and Horvitz 1991), and it is therefore reasonable to expect that proper cilia in these amphid neurons might be important for their function even in dauer larvae. In Chlamydomonas, cessation of IFT results in foreshortening of the flagellum (for review, see Rosenbaum and Witman 2002). It is not clear if a similar foreshortening of cilia would occur in *C. elegans* if IFT were stopped postembryonically, because the cilia are not in free structures. They are embedded in a supporting structure in a channel that penetrates the body wall. The dendritic endings of the left and right ASG and ASI neurons have been reported to be slightly retracted in the amphid channels of dauer larvae (Albert and Riddle 1983). It is interesting in this regard that there appeared to be fewer GFP particles undergoing IFT in the amphid channels of dauer larvae relative to non-dauer animals. Perhaps this impression reflects a reduction of IFT in ASG and ASI, which results in their retraction, but this notion is highly speculative at this stage.

IFT is maintained constantly throughout development and the life cycle (for review, see Rosenbaum and Witman 2002). Genetic analyses in Chlamydomonas

and *C. elegans* strongly indicate that IFT is required for the assembly and maintenance of the flagellar and ciliary axoneme. It has been argued also that IFT is a means of transporting other cytoplasmic components, including those needed for reception of extracellular signals, within these structures. We suggest another possibility—that IFT plays a general role as a circulatory system for the cilia and flagella. The constancy of IFT may reflect the necessity of providing ATP and other essential components to a long cylinder of narrow diameter at the termini of dendrites, which are themselves long and narrow. In any case, the defective, foreshortened dendritic endings present in *dyf-6* mutants, as visualized with OSM-6::GFP, further strengthen the correlation between functional IFT and proper structure of cilia.

We thank the following: Lihsia Chen for use of her microscope, for help with the time-lapse microscopy, and for support of J.Y. during the final stages of this work; Margaret Titus and Laura Breshears for help with processing time-lapse images; Don Riddle for alleles from the mutator strain; Chris Link for the phage genomic library; Stuart Kim, H. R. Horvitz, Bob Barstead, and Bob Waterston for cDNA libraries; John Sulston and Alan Coulson for DNA fingerprint analysis of λ-clones; Alan Coulson for cosmid clones; and Andrew Fire and colleagues for the GFP expression vector. Some nematode strains were supplied by the Caenorhabditis Genetics Center, which is supported by a contract between the National Institutes of Health National Center for Research Resources and the University of Minnesota. Support was from National Institutes of Health grants GM-22387 and HD-22163.

LITERATURE CITED

Albert, P. S., and D. L. Riddle, 1983 Developmental alterations in sensory neuroanatomy of the *Caenorhabditis elegans* dauer larva. J. Comp. Neurol. **219:** 461–481.

Albert, P. S., S. J. Brown and D. L. Riddle, 1981 Sensory control of dauer larva formation in *Caenorhabditis elegans*. J. Comp. Neurol. **198:** 435–451.

Altschul, S. F., T. L. Madden, A. A. Schaffer, J. Zhang, Z. Zhang *et al.*, 1997 Gapped BLAST and PSI-BLAST: a new generation of protein database search programs. Nucleic Acids Res. **25:** 3389–3402.

Avidor-Reiss, T., A. M. Maer, E. Koundakjian, A. Polyanovsky, T. Keil *et al.*, 2004 Decoding cilia function: defining specialized genes required for compartmentalized cilia biogenesis. Cell **117:** 527–539.

Bargmann, C. I., and H. R. Horvitz, 1991 Control of larval development by chemosensory neurons in *Caenorhabditis elegans*. Science **251:** 1243–1246.

Blacque, O. E., E. A. Perens, K. A. Boroevich, P. N. Inglis, C. Li *et al.*, 2005 Functional genomics of the cilium, a sensory organelle. Curr. Biol. **15:** 935–941.

Cole, D. G., 2003 The intraflagellar transport machinery of *Chlamydomonas reinhardtii*. Traffic **4:** 435–442.

Cole, D. G., 2005 Intraflagellar transport: keeping the motors coordinated. Curr. Biol. **15:** R798–R801.

Cole, D. G., D. R. Diener, A. L. Himelblau, P. L. Beech, J. C. Fuster *et al.*, 1998 *Chlamydomonas* kinesin-II-dependent intraflagellar transport (IFT): IFT particles contain proteins required for ciliary assembly in *Caenorhabditis elegans* sensory neurons. J. Cell Biol. **141:** 993–1008.

Collet, J., C. A. Spike, E. A. Lundquist, J. E. Shaw and R. K. Herman, 1998 Analysis of *osm-6*, a gene that affects sensory cilium structure and sensory neuron function in *Caenorhabditis elegans*. Genetics **148:** 187–200.

Efimenko, E., K. Bubb, H. Y. Mak, T. Holzman, M. R. Leroux *et al.*, 2005 Analysis of *xbx* genes in *C. elegans*. Development **132:** 1923–1934.

Herman, R. K., and E. M. Hedgecock, 1990 Limitation of the size of the vulval primordium of *Caenorhabditis elegans* by *lin-15* expression in surrounding hypodermis. Nature **348:** 169–171.

Lewis, J. A., and J. A. Hodgkin, 1977 Specific neuroanatomical changes in chemosensory mutants of the nematode *Caenorhabditis elegans*. J. Comp. Neurol. **172:** 489–510.

Li, J. B., J. M. Gerdes, C. J. Haycraft, Y. Fan, T. M. Teslovich *et al.*, 2004 Comparative genomics identifies a flagellar and basal body proteome that includes the *BBS5* human disease gene. Cell **117:** 541–552.

Mello, C., and A. Fire, 1995 DNA transformation. Methods Cell. Biol. **48:** 451–482.

Mello, C. C., J. M. Kramer, D. Stinchcomb and V. Ambros, 1991 Efficient gene transfer in *C. elegans*: extrachromosomal maintenance and integration of transforming sequences. EMBO J. **10:** 3959–3970.

Murayama, T., Y. Toh, Y. Ohshima and M. Koga, 2005 The *dyf-3* gene encodes a novel protein required for sensory cilium formation in *Caenorhabditis elegans*. J. Mol. Biol. **346:** 677–687.

Orozco, J. T., K. P. Wedaman, D. Signor, H. Brown, L. Rose *et al.*, 1999 Movement of motor and cargo along cilia. Nature **398:** 674.

Ou, G., O. E. Blacque, J. J. Snow, M. R. Leroux and J. M. Scholey, 2005a Functional coordination of intraflagellar transport motors. Nature **436:** 583–587.

Ou, G., H. Qin, J. L. Rosenbaum and J. M. Scholey, 2005b The PKD protein qilin undergoes intraflagellar transport. Curr. Biol. **15:** R410–R411.

Pedersen, L. B., M. S. Miller, S. Geimer, J. M. Leitch, J. L. Rosenbaum *et al.*, 2005 Chlamydomonas IFT172 is encoded by *FLA11*, interacts with CrEB1, and regulates IFT at the flagellar tip. Curr. Biol. **15:** 262–266.

Perkins, L. A., E. M. Hedgecock, J. N. Thomson and J. G. Culotti, 1986 Mutant sensory cilia in the nematode *Caenorhabditis elegans*. Dev. Biol. **117:** 456–487.

Piperno, G., E. Siuda, S. Henderson, M. Segil, H. Vaananen *et al.*, 1998 Distinct mutants of retrograde intraflagellar transport (IFT) share similar morphological and molecular defects. J. Cell Biol. **143:** 1591–1601.

Qin, H., J. L. Rosenbaum and M. M. Barr, 2001 An autosomal recessive polycystic kidney disease gene homolog is involved in intraflagellar transport in *C. elegans* ciliated sensory neurons. Curr. Biol. **11:** 457–461.

Riddle, D. L., and P. S. Albert, 1997 Genetic and environmental regulation of dauer larva development, pp. 739–768 in *C. elegans II*, edited by D. L. Riddle, T. Blumenthal, B. J. Meyer and J. R. Priess. Cold Spring Harbor Laboratory Press, Plainview, NY.

Rosenbaum, J. L., and G. B. Witman, 2002 Intraflagellar transport. Nat. Rev. Mol. Cell Biol. **3:** 813–825.

Scholey, J. M., 2003 Intraflagellar transport. Annu. Rev. Cell Dev. Biol. **19:** 423–443.

Signor, D., K. P. Wedaman, J. T. Orozco, N. D. Dwyer, C. I. Bargmann *et al.*, 1999 Role of a class DHC1b dynein in retrograde transport of IFT motors and IFT raft particles along cilia, but not dendrites, in chemosensory neurons of living *Caenorhabditis elegans*. J. Cell Biol. **147:** 519–530.

Sloboda, R. D., 2005 Intraflagellar transport and the flagellar tip complex. J. Cell. Biochem. **94:** 266–272.

Smith, T. F., C. Gaitatzes, K. Saxena and E. J. Neer, 1999 The WD repeat: a common architecture for diverse functions. Trends Biochem. Sci. **24:** 181–185.

Snow, J. J., G. Ou, A. L. Gunnarson, M. R. Walker, H. M. Zhou *et al.*, 2004 Two anterograde intraflagellar transport motors cooperate to build sensory cilia on *C. elegans* neurons. Nat. Cell Biol. **6:** 1109–1113.

Starich, T. A., R. K. Herman, C. K. Kari, W. H. Yeh, W. S. Schackwitz *et al.*, 1995 Mutations affecting the chemosensory neurons of *Caenorhabditis elegans*. Genetics **139:** 171–188.

Sulston, J. E., E. Schierenberg, J. G. White and J. N. Thomson, 1983 The embryonic cell lineage of the nematode *Caenorhabditis elegans*. Dev. Biol. **100:** 64–119.

Ward, S., N. Thomson, J. G. White and S. Brenner, 1975 Electron microscopical reconstruction of the anterior sensory anatomy of the nematode *Caenorhabditis elegans*. J. Comp. Neurol. **160:** 313–337.

Ware, R. W., D. Clark, K. Crossland and R. L. Russel, 1975 The nerve ring of the nematode *Caenorhabditis elegans:* sensory input and motor output. J. Comp. Neurol. **162:** 71–110.

White, J. G., E. Southgate, J. N. Thomson and S. Brenner, 1986 The structure of the nervous system of the nematode *Caenorhabditis elegans*. Philos. Trans. R. Soc. Lond. B Biol. Sci. **314:** 1–340.

Yochem, J., T. Gu and M. Han, 1998 A new marker for mosaic analysis in *Caenorhabditis elegans* indicates a fusion between hyp6 and hyp7, two major components of the hypodermis. Genetics **149:** 1323–1334.

Communicating editor: K. Kemphues